Presented in International Symposium on Photovoltaic Science and Technology, Indian Institute of Technology, Kanpur, 13 January, 2010

Photovoltaic Energy Conversion System for Water Pumping Applications – Modeling and Simulation

B.Chitti Babu, R. Sudharshan Kaarthik, Nayan Kumar Dalei, R.Vigneshwaran, Rabi Narayan Das
Department of Electrical Engineering, National Institute of Technology, Rourkela, INDIA
E-mail: bcbabu@nitrkl.ac.in, sudharshan.kaarthik@gmail.com, nayandalei@gmail.com, vigneshnitj@gmail.com

Abstract**: In this paper, dynamic modeling and simulation of photovoltaic energy conversion system for water pumping application is presented. The proposed system include the dynamic modeling of the photovoltaic (PV) cells with the effects of solar irradiation and temperature changes, model of the DC to DC boost converter, inductor design procedure for boost converter and model of the single phase IGBT based sinusoidal PWM voltage source inverter. The whole system has been developed and simulated using Matlab-Simulink environment via graphical user interface. The simulated results are validated with theoretical results and we find proper synchronism between the two results.**

Index Terms: **Boost Converter, Inductor design, Photo voltaic Array, PWM inverter.**

I. INTRODUCTION

The use of new efficient photovoltaic solar cells (PVSCs) has emerged as an alternative measure of renewable green power, energy conservation and demand-side management. Owing to their high initial cost, PVSCs have not yet been fully an attractive alternative for electricity users who are able to buy cheaper electrical power from the utility grid. However, they can be used extensively for water pumping and air conditioning in remote and isolated areas, where utility power is not available or is too expensive to transport [1].

This paper presents a single system to convert photovoltaic power to useable single phase AC at 230 V to drive a fractional horse power induction motor for water pumping application [2-3]. The power obtained from the solar cell is unusable as it is a low voltage power (approx. 24 V, 720 W) and is DC. However, for water pumping application we need 230V single phase AC supply. The 24V DC obtained from the PV array is boosted up to 325V by a DC-DC boost converter. The design of the inductor in the boost converter circuit is the most important step in the design of the converter. The DC power available at the output of boost converter is filtered and is converted to AC power using voltage source inverter which employs sinusoidal PWM. The single-phase PWM inverter is simulated and the corresponding firing pulses are produced to trigger the IGBT switches. In the SPWM scheme, a carrier wave is compared with the reference signal corresponding to single-phase to generate the gating pulses for the concerned switches with the switching frequency of 10 KHz, with the rated output voltage of 230 volts. The rated inverter voltage of 280 volts is obtained for the modulation index of 0.9. The whole system has been developed and simulated using Matlab-Simulink environment via graphical user interface. The simulated results are validated with theoretical results and we find the proper synchronism between the two results.

II. PHOTOVOLTAIC ARRAY SIMULATION

A. PVA Modeling

During the design process of PVA powered systems, a simulation must be performed for system analysis and parameter settings. Therefore an efficient user-friendly simulation model of the PVAs is always needed. The PVA model proposed in this paper is a circuit based model to be used with Simulink. The proposed model was simulated with various types of loads for performance checking.

PV arrays are built up with combined series/parallel combinations of PV solar cells, which are usually represented by a simplified equivalent circuit model such as the one given in Fig. 1 or by eq.(1) [4].

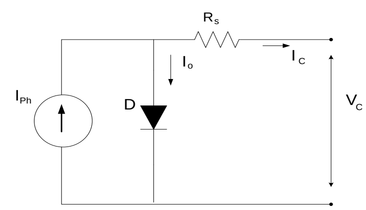

Fig. 1. Simplified equivalent circuit of PV cell

The PV cell output voltage is a function of the photocurrent which is mainly determined by the load current and the solar radiation level during the operation.

$$V_c = \frac{AkT_c}{e}\, ln\left\{\frac{I_{ph}+I_0-I_c}{I_0}\right\} - R_s I_c \tag{1}$$

where the symbols are defined as follows:

e : electron charge (1.602×10^{-19} °C)
k : Boltzmann constant (1.38×10^{-23} J/K)
I_c : Cell output current, A
I_{ph}: Photocurrent - a function of irradiation level and junction temperature, A
I_0 : Reverse saturation current of diode (0.0002 A).
R_s: Series resistance of cell (0.001 Ω).
T_c: Reference cell operating temperature (20 °C).
V_c: Cell output voltage, V.

Both k and T_c should have the same temperature unit, i.e. ℃ or Kelvin. The curve fitting factor A is used to adjust the *I-V* characteristics of the cell obtained from eq.(1) to the actual characteristics obtained by testing. Equation(1) gives the voltage of a single solar cell which is then multiplied by the number of the cells connected in series to calculate the full array voltage. Since the array current is the sum of the currents flowing through the cells in parallel branches, the cell current I_C is obtained by dividing the array current by the number of cells connected in parallel before being used in eq.(1), which is only valid for a certain operating temperature T_c with its corresponding solar irradiation level S_c. If the temperature and solar irradiation level changes, the voltage and current output of the PV array will follow this change. Hence, the effects of the changes in temperature and solar irradiation levels should be included in the final PV array model.

B. Temperature and Irradiation Correction factors

For a known temperature and a known solar irradiation level, a model is obtained and then this model is modified to handle different cases of temperatures and irradiation levels. Let eq.(1) be the benchmark model for the known operating temperature T_c and known solar irradiation level S_c as given in the specification. When the ambient temperature and irradiation level changes, the cell operating temperature also changes, resulting in a new output voltage and a new photocurrent value. The solar cell operating temperature varies as a function of solar irradiation level and ambient temperature. The ambient temperature T_a affects the cell output voltage and cell photocurrent. These effects are represented in the model by the temperature coefficients C_{TV} and C_{TI} for cell output voltage and cell photocurrent, respectively, as

$$C_{TV} = 1 + \beta_T (T_a - T_x) \tag{2}$$

$$C_{TI} = 1 + \frac{\gamma_T}{S_C} (T_a - T_x) \tag{3}$$

where, β_T = 0.004 and γ_T = 0.06 for the cell used and T_a=20˚C is the ambient temperature during the cell testing. This is used to obtain the modified model of the cell for another ambient temperature T_x. Even if the ambient temperature does not change significantly during the daytime, the solar irradiation level changes depending on the sunlight and clouds. A change in solar irradiation level causes a change in the cell photocurrent and operating temperature, which in turn affects the cell output voltage. If the solar irradiation level increases from S_{x1} to S_{x2}, the cell operating temperature and the photocurrent will increase from T_{x1} to T_{x2} and from I_{phl} to I_{ph2}, respectively. Thus the change in the operating temperature and the photocurrent due to variation in the solar irradiation level can be expressed with the help of two constants, C_{SV} and C_{SI}, which are the correction factors for changes in cell output voltage V_C and photocurrent I_{ph}, respectively.

$$C_{SV} = 1 + \beta_T \alpha_S (S_x - S_c) \tag{4}$$

$$C_{SI} = \frac{1}{S_C} (S_x - S_c) \tag{5}$$

where, S_c is the benchmark reference solar irradiation level during the cell testing. S_x is the new level of the solar irradiation. The temperature change ΔT_C occurs due to the change in the solar irradiation level which is obtained using

$$\Delta T_c = \alpha_S (S_x - S_c) \tag{6}$$

The constant α_S represents the slope of the change in the cell operating temperature due to a change in the solar irradiation level and is equal to 0.2 for the PVA used. Using correction factors C_{TV}, C_{TI}, C_{SV} and C_{SI}, the new values of the cell output voltage V_{Cx} and photocurrent I_{phx} are obtained for the new temperature T_x and solar irradiation S_x

.

$$V_{CX} = C_{SV}\, C_{TV}\, V_C \tag{7}$$

$$I_{phx} = C_{SI}\, C_{TI}\, I_{ph} \tag{8}$$

V_C and I_{ph} are the benchmark reference cell output voltage and reference cell photocurrent, respectively. The final model of the PV Array is shown in the discussion section.

III. The Boost Converter

Boost converters make it possible to efficiently convert a DC voltage from a lower level to a higher level [5]. The fig. 2 depicts a step up boost converter. It consists of a DC input voltage source V_S, boost inductor L, controlled switch S, diode D, filter capacitor C, and load resistance R.

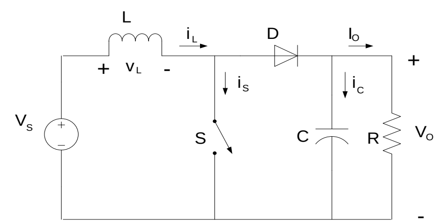

Fig. 2. Boost Converter

The switch S is replaced with a MOSFET. Diode D is a Schottky diode. Schottky diode offers a very small recovery period with a minimum voltage drop across it during ON period. The metal-semiconductor junction is responsible for the low voltage drop. Design of the inductor L is very important and critical step in the Boost Converter design. The design procedure is explained in the following section.

IV. Inductor Design

A. Relation between V_{out} and V_{in} in Continuous Conduction

The idealized boost converter circuit is shown below in figure 3. Under normal operation, the circuit is in *continuous conduction mode* (i.e., i_L is never zero) [6].

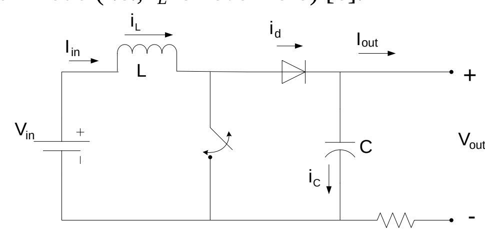

Fig. 3. DC - DC Boost Converter

The circuit is assumed to be lossless so that $P_{in} = P_{out}$ or, $V_{in}\, I_{Lavg} = V_{out}\, I_{out}$ where I_{Lavg}=I_{in}.

Assuming continuous conduction, the circuit has two states switch closed, and switch open. They are shown in figures 4 and 5.

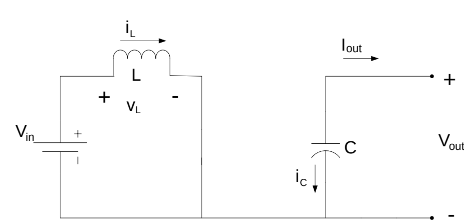

Fig. 4. Switch Closed

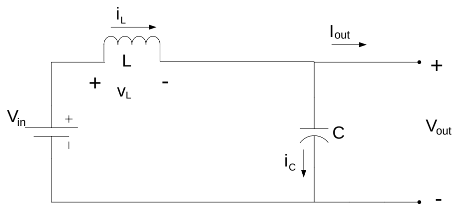

Fig. 5. Switch Open

When the switch is closed, the diode is reverse biased and open, I_L increases at the rate of

$$\frac{d\, i_L}{dt} = \frac{V_L}{L} = \frac{V_{in}}{L} \;, 0 \le t \le DT \qquad (9)$$

and the inductor is *charging*. When the switch is open, the diode is forward biased, i_L decreases at the rate of

$$\frac{d\, i_L}{dt} = \frac{V_L}{L} = \frac{V_{in} - V_{out}}{L} \;, DT \le t \le T \qquad (10)$$

and the inductor is *discharging*. The inductor voltage is shown in figure 6.

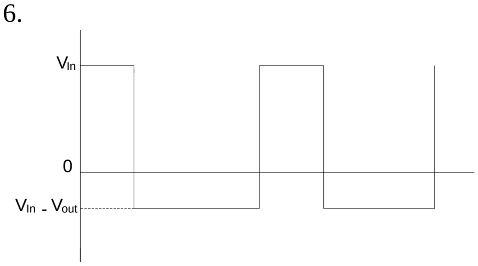

Fig. 6. Inductor Voltage

Because of the steady-state inductor principle, the average voltage V_L across L is zero. Since v_L has two states, both having constant voltage, the average value is

$$\frac{V_{in}(DT) + (V_{in} - V_{out})(1-D)T}{T} = 0 \qquad (11)$$

The above expression reduced to

$$V_{out} = \frac{V_{in}}{1-D} \qquad (12)$$

B. Inductor current in continuous conduction

The graph of i_L is shown in figure 7.

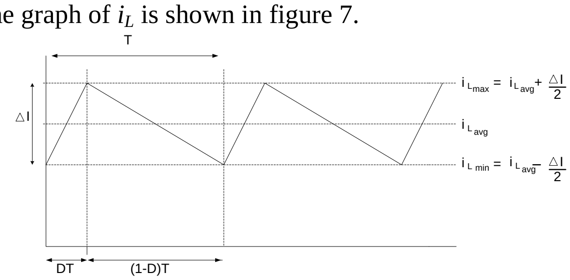

Fig. 7. Inductor Current

From equation 9 and the boundary condition I_{Lmin}=0,

$$\Delta I = \frac{(V_{out} - V_{in})(1-D)}{L_{boundary}\;\; f} = \frac{V_{in} - V_{in}(1-D)}{L_{boundary}\;\; f} = \frac{V_{in} D}{L_{boundary}\;\; f} = 2 I_{L\,avg}, \qquad (13)$$

so that

$$L_{boundary} = L_{crit} = \frac{V_{in} D}{2 I_{L\,avg} f} = \frac{V_{in} D}{2 I_{in} f} \qquad (14)$$

will guarantee continuous conduction for all D. The inductor is designed for specific scheme in this paper.

C. Inductor Design

The design procedure starts with the determination of the input states of the inductor which are also the input parameters for the design. The selection of topology, power developed P_{out}, switching frequency f_{SW}, output DC voltage V_{out}, minimum input voltage $V_{in\ min}$, maximum input voltage $V_{in\ max}$, maximum temperature T, efficiency of the inductor η_L, efficiency of the pre-regulator η_{preg} are the required parameters for the design problem.

The equations used to design the inductor are given below.

$$P_{tot} = (1 - \eta_L)(P_{out} / \eta_{p\ reg})\ Watts \qquad (15)$$

$$P_{core} = {P_{tot}}/{2} = P_{cu}\ \ Watts \qquad (16)$$

Loss per core weight is given by

$$p_i = \frac{P_{tot}}{2\, wt}\ Watts\ per\ kg \qquad (17)$$

Core loss is also equal to

$$P = 6.5\, f_{SW}^{1.51}\ B_{ac}^{1.74}\ Watts \qquad (18)$$

Having calculated the L_{crit} and I_{in} we now calculate the energy storage requirements of the inductor.

$$E = 0.5(L_{crit}\, I_{in\ peak}^2)\ Watts \qquad (19)$$

The required area product W_aA_c is given by

$$W_a A_c = \frac{2E \times 10^4}{B_{max}\ J\ K}\ cm^2 \qquad (20)$$

where, J is the current density and K is the window utilization factor. The number of turns and the air-gap required is given by the following expressions.

$$N = \frac{L_{crit}\, I_{in\ crit} \times 10^4}{B_{max}\ A_c} \qquad (21)$$

$$l_g = \frac{0.4\,\pi\, N\, I_{in\ pk} \times 10^{-4}}{B_{max}} - \frac{l_m}{\mu\Delta}\ cm \qquad (22)$$

where l_m is the magnetic mean length and $\mu\Delta$ is the incremental magnetic permeability of the core material. The core can be selected using the catalogue from the manufacturers. The details to be obtained from the manufacturers are the core dimensions a, b, c, d, e, f, l_m, area A_c, surface area SA. Refer to fig. 8 for the dimensions of the core. The conductor area and the losses can be calculated by taking current density and resistivity of copper into account.

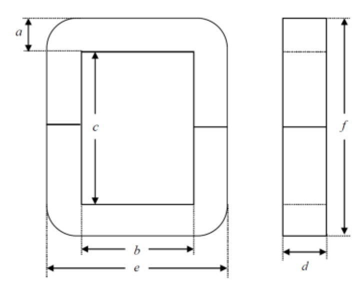

Fig. 8. Core dimensions of inductor

The MATLAB code for the design of inductor is given in Appendix 1.

V. INVERTER

The input to the inverter is the output from the Boost Converter. It is 325V DC power. The inverter proposed is an IGBT based single phase sinusoidal pulse width modulated voltage source inverter.

The main objective of static power converters is to produce an AC output waveform from a DC power supply [7]. These are the types of waveforms required in adjustable speed drives

(ASDs), uninterruptible power supplies (UPS), static VAR compensators, active filters, flexible AC transmission systems (FACTS) and voltage compensators which are only a few applications. For sinusoidal AC outputs, the magnitude, the frequency, and the phase should be controllable.

The Single phase full bridge voltage source inverter is shown in figure 9.

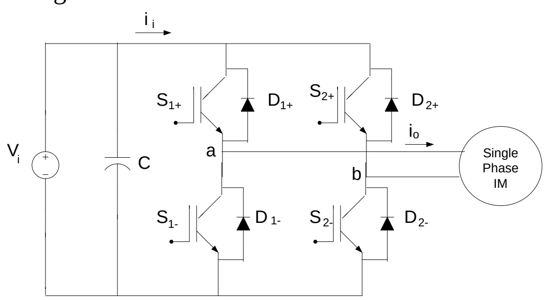

Fig. 9. Single Phase Full Bridge VSI

Uni-polar PWM inverters (also known as Class D or switching amplifiers) efficiently amplify a small input signal V_{cont}. The output voltage to the load is either $+V_{dc}$, $-V_{dc}$, or zero, depending on whether V_{cont} or $-V_{cont}$ is greater or smaller than a reference triangle wave V_{tri}. The output load voltage contains a replica of V_{cont}, and also strong harmonics around even multiples of m_f, where m_f is the ratio of the reference triangle wave frequency with respect to the frequency of V_{cont}.

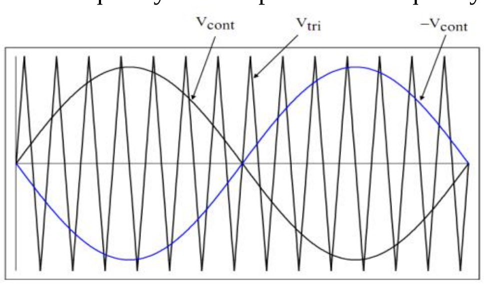

Fig. 10. Waveforms of Sine wave and Triangle wave

The illustration in fig. 10 has $m_a = 0.9$, where m_a is the ratio of peak control voltage to peak triangle (modulation index).

A high-frequency signal is compared with a specific sinusoidal signal with specific frequency. The high-frequency signal is known as carrier or modulator signal. The carrier can be a triangular train of pulses shown in fig. 10. This minimizes the noise in the system, ripple current, harmonic distortion and acoustic noise. In the SPWM the reference signal is a sinusoid [8–10]. The comparison of this signal with triangular wave generates the output as shown in fig. 11. In order to make the analysis of SPWM it is necessary to define some parameters namely m_f and m_a.

$$m_f = \frac{f_{tri}}{f_{cont}} \tag{23}$$

$$m_a = \frac{V_{Cont}}{V_{Tri}} \tag{24}$$

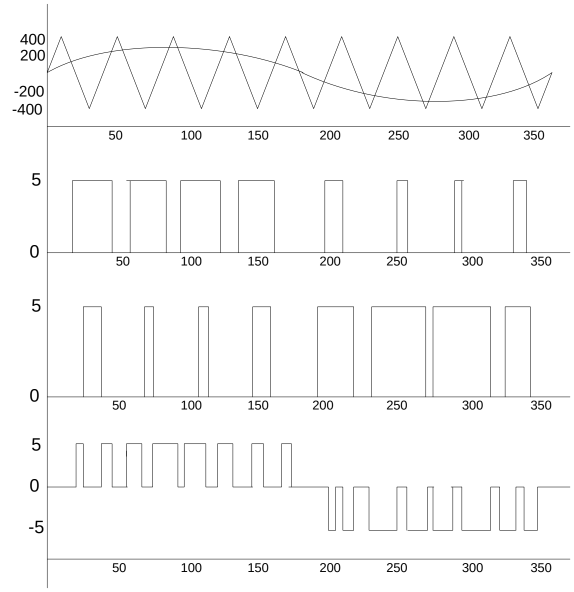

Fig. 11. SPWM Modulation

VI. Modeling of PVA Using Simulink

The Simulink block diagram is shown in the figure 12. Figures 13 and 14 show the incorporation of correction factors to the developed model.

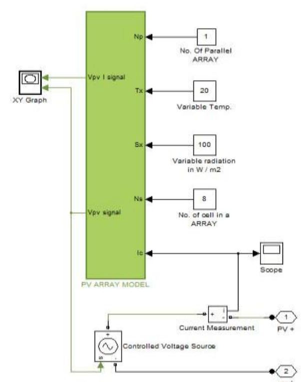

Fig. 12. Functional block diagram of PVA

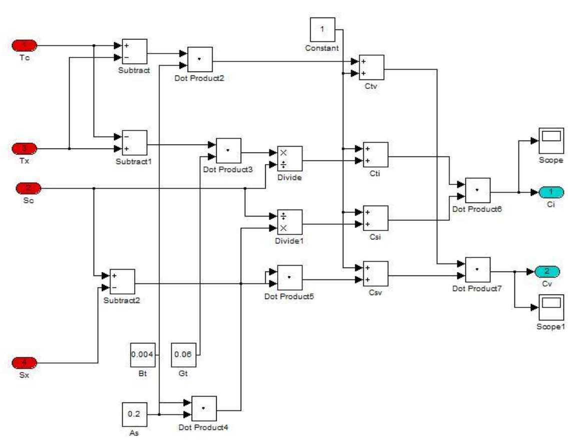

Fig. 13. Sub System for Correction factors

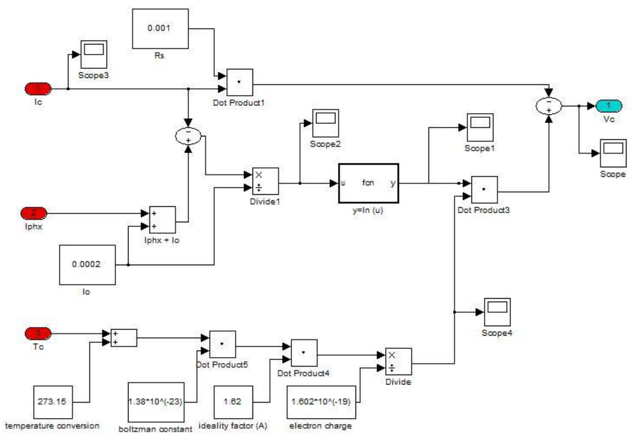

Fig. 14. Sub System for Correction factors

This model proposes fifteen cells in series and four such arrays in parallel. The assumed ambient temperature is 20˚C and the light intensity is 100W/m^2.

VII. Simulation of the Boost Converter and Inverter

The Simulink model for converter is shown in the fig. 15 and the inverter in fig. 16. The value of reactive power required by inductor is 214.52 VAR at a nominal voltage level of 280 V.

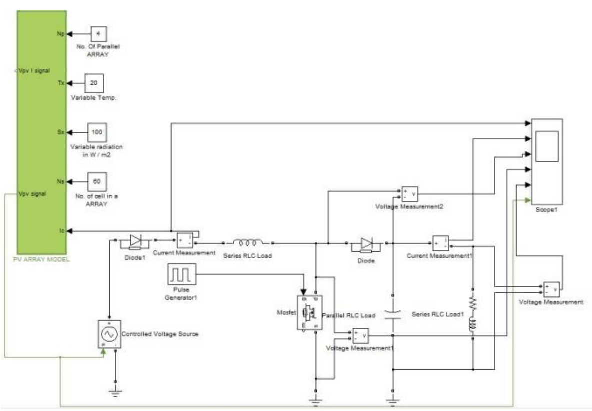

Fig. 15. Boost Converter model

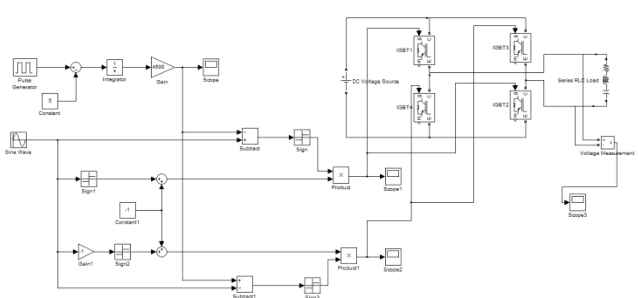
Fig. 16. SPWM based VSI model in Simulink

The simulation results are presented in the Results and Discussion section.

VIII. Results and Discussion

The fig.17 shows the current versus voltage graph for the simulated photo voltaic array. As the open circuit condition clearly describes a zero current, the value of voltage at that point gives the value of open circuit voltage of the array or cell. Moreover, the short circuit condition is where the voltage becomes zero. This value of current is very important as it helps on suggestion of the optimum value of current drawn for maximum power. Note that the value of the current increases for rise in the temperature.

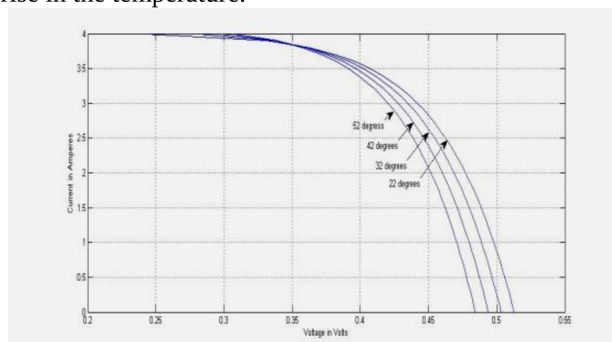

Fig. 17. Current Vs Voltage of PV Array

The figure 18 shows the power versus voltage graph. This graph is plotted for various temperatures. We can see that the maximum output power decreases with increase in temperature.

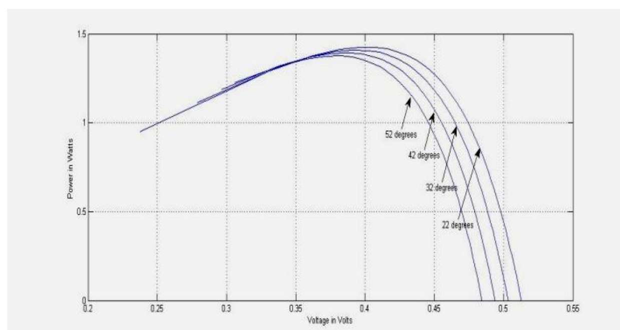

Fig. 18. Power Vs Voltage of PV Array

Figure 19 shows the outputs of the boost converter. 19(a) shows the input current to the boost converter. 19(b) shows the output current of the converter. 19(c) shows the voltage across Schottky diode, 19(d) the voltage across MOSFET, 19(e) is the output voltage of the Boost Converter and 19(f) is the output voltage of the photovoltaic array which is also the input to the converter.

The output of the inverter is shown in figure 19. The SPWM can be clearly seen for a modulation index of 0.90.

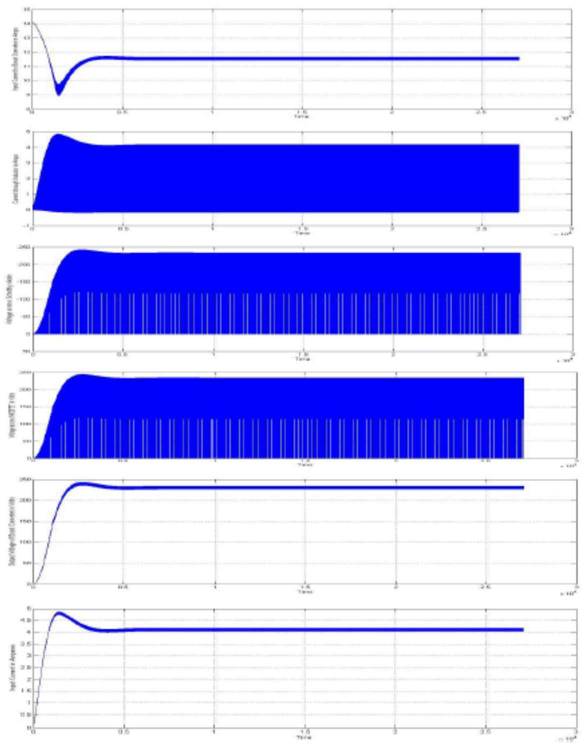

Fig.19. (a)Input current to the boost converter (b) Output current of the converter (c) Voltage across Schottky diode (d) Voltage across MOSFET (e)Output voltage of the Boost Converter (f)Output voltage of the photovoltaic array

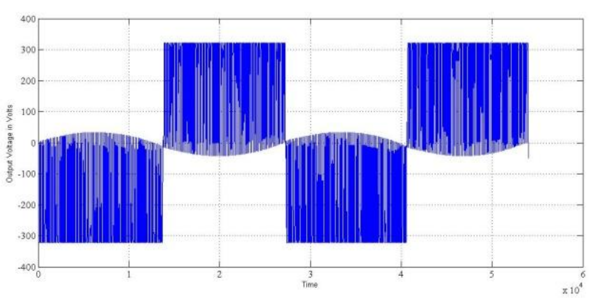

Fig. 20. Output voltage of the single phase VSI

IX. CONCLUSION

The photovoltaic array has been modeled and GUI has been developed in the Simulink environment. An economical converter system for converting the output from PV panels into 50Hz AC voltage is presented. The boost converter helps to provide a regulated DC voltage that is then converted into a single phase AC voltage by SPWM VSI. Moreover, the design of inductor for dc-dc boost converter has been computed through computer simulation in an effective way. The MOSFET switch in the boost converter can also provide control signal for maximum power point tracking and it will be focused in the future work.. The inverter output wave-form has only higher order harmonics and that can be easily eliminated by LC filter on the load side.

X. APPENDIX

A. *MATLAB code for indctor design*

```
function myinductor(Lcrit,Icrit,Pout,fsw,Vout,
Vin,Vinmax,temp,NL,Npreg)
Ptot=(1-NL)*(Pout/Npreg)
Pcore=Ptot/2
%using AMCC-25 core at 50 degrees
wt=22.2
P=Ptot/(2*wt)
Bmax=1.3
Bac=(P/(6.5*fsw^1.51))^(1/1.74)
delB=2*Bac
delI=(delB/Bmax)*(sqrt(2)*Pout/(Npreg*Vin))
delILcrit=(sqrt(2)*Vin*(1-sqrt(2)*Vin/Vout))/(delI*fsw)
E=0.5*Lcrit*Icrit^2
J=500
K=0.4
WaAc=2*E*10000/(Bmax*J*K)
%refering to manufacturer's catalogue
a=1.3; b=1.5; c=5.6; d=2.5; e=4; f=8.2;
lm=19.6
Ac=2.7
mudelta=1000
N=round((Lcrit*Icrit*10000)/(Bmax*Ac))
lg=0.4*pi*N*Icrit*(10^-4)/Bmax-lm/mudelta
F=(a+lg)*(d+lg)/(a*d)
Ncorrect=sqrt((Lcrit*(lg+(lm/mudelta))*10^8)/(0/4*pi*Ac*F))
Ncorrect=round(Ncorrect)
Ax=b*c*K/N
Runit=2.16/Ax
MTL=2*(a+2*b+d)*10^-4
ResTotal=Runit*MTL*N
Pcu=Icrit^2*ResTotal
Bac=0.4*pi*Ncorrect*(delILcrit/2*10^-4)/lg
SA=2*f*(b+d)+2*(b+d)*(b+e)+2*f*(b+e)
delT=(Ptot/SA)^0.833
```

REFERENCES

[1] S.Yuvarajan, Dachuan Yu and Shanguang Xu, "A novel power converter for photo voltaic applications" Elsevier Journal of Power Sources, June-2004.
[2] Y. Kuo, et al., Maximum-power-point-tracking controller for photo-voltaic energy conversion system, IEEE Trans. Ind. Electron. 48 (3) (2001) 594–601.
[3] M.R. Patel, Wind and Solar Power Systems, CRC Press, 1999.
[4] D.L. King, J.H. Dudley, W.E. Boyson, PVSIM: a simulation program for photovoltaic cells, modules and arrays, in: Proceedings of the 25th IEEE Photovoltaic Specialists Conference, May 1996.
[5] D.L. King, et al., Field experience with a new performance characterization procedure for photovoltaic arrays, in: Proceedings of the Second World Conference on Photovoltaic Solar Energy Conversion, July 1998.
[6] I. H. Altas, and A.M. Sharaf, A Photovoltaic Array Simulation Model for Matlab-Simulink GUI Environment, 1-4244-0632-3/07 IEEE.
[7] C.G. Steyn, Analysis and optimization of regenerative linear snubbers, IEEE Trans. Power Electron 4 (3) (1989) 362–370.
[8] M. Buresch: Photovoltaic Energy Systems Design and Installation,McGraw-Hill, New York, 1983.
[9] I. H. Altas and A.M. Sharaf: A Novel On-Line MPP Search Algorithm for PV Arrays, IEEE Transactions on Energy Conversion, Vol. 11, No.4, December 1996, pp. 748-754.
[10] K. Benlarbi, L. Mokrani, M.S. Nait-Said: A fuzzy global efficiency optimization of a photovoltaic water pumping system, Solar Energy, 77 (2004) 203–216.